Supplement of Atmos. Chem. Phys., 22, 561–575, 2022
https://doi.org/10.5194/acp-22-561-2022-supplement

Atmospheric Chemistry and Physics
Open Access

Supplement of

Measurement report: Long-term changes in black carbon and aerosol optical properties from 2012 to 2020 in Beijing, China

Jiaxing Sun et al.

Correspondence to: Yele Sun (sunyele@mail.iap.ac.cn)

Estimation of ΔF_R uncertainty

The uncertainties of BC and BrC ΔF_R (including primary and secondary ones) were quantitatively determined using Monte Carlo simulations. Note that the uncertainty was expressed as one standard deviation (±1σ) or the coefficient of variation (CV, σ divided by the mean) as a percentage. According to the uncertainty propagation, the CV for $b_{abs, BC}$ (λ) is:

$$CV_{b_{abs,BC(\lambda)}} \approx \sqrt{\left[(CV_{b_{abs,BC,880}})^2 + [CV_\alpha * \alpha * (\ln\frac{880}{\lambda})]^2\right]} \qquad (1)$$

where $CV_{babs, BC, 880}$ and CV_α represent the uncertainty of measured absorption coefficient at 880nm (~ 25%) and absorption Ångström exponent of pure BC (~ 10%) (Gyawali et al., 2009; Bond et al., 2013; Lack and Langridge, 2013; Lu et al., 2015), respectively. The CV for $b_{abs, BrC}$ (λ) could be quantified as:

$$CV_{b_{abs,BrC,370}} \approx \sqrt{\left[(CV_{b_{abs,total,370}})^2 + [CV_\alpha * \alpha * (\ln\frac{880}{370})]^2\right]} \qquad (2)$$

$$CV_{b_{abs,BrC(\lambda)}} \approx \sqrt{\left[(CV_{b_{abs,BrC,370}})^2 + [CV_\beta * \beta * (\ln\frac{370}{\lambda})]^2\right]} \qquad (3)$$

where $CV_{babs, BrC, 370}$ (~26%) and CV_β represent the uncertainties of BrC absorption coefficient at 370 nm and absorption Ångström exponent of BrC (fitting uncertainty ~ 10%), respectively. Similarly, $CV_{babs, PriBrC, (\lambda)}$ and $CV_{babs, SecBrC(\lambda)}$ could also be quantified. Then we applied normal distributions for measured data with uncertainties provided by the calculated CVs and 100 000 simulations by Monte Carlo analysis. After running the radiative forcing model repeatedly, we got 100 000 RF values, and the standard deviation could be considered as the uncertainty of radiative forcing. The probability distributions of ΔF_R for BC and different types of BrC are shown in Fig. S12. The uncertainties of BC and BrC absorption ΔF_R are comparably about 27 ~ 28%. And the uncertainties for primary and secondary BrC absorption ΔF_R are about 32% and 43%, respectively.

Table S1. A summary of Mann-Kendall trend test for air pollutants from 2013 to 2020.

	Entire	Spring	Summer	Fall	Winter
	τ (p-value)	τ (p-value)	τ (p-value)	τ (p-value)	τ (p-value)
eBC	**-1** **(0.01)**	**-1** **(0.01)**	-0.4 (0.33)	**-1** **(0.01)**	-0.4 (0.33)
eBC/$PM_{2.5}$	-0.6 (0.14)	0.4 (0.33)	-0.4 (0.33)	**-0.8** **(0.05)**	**-0.8** **(0.05)**
eBC/CO	-0.6 (0.14)	**-0.8** **(0.05)**	-0.4 (0.33)	-0.6 (0.14)	**-0.8** **(0.05)**
b_{ext}	**-0.8** **(0.05)**	**-0.8** **(0.05)**	- -	**-0.8** **(0.05)**	-0.4 (0.33)
SSA	**1** **(0.01)**	- -	**0.8** **(0.05)**	**0.8** **(0.05)**	**0.8** **(0.05)**
MEE	0.4 (0.33)	-0.2 (0.62)	**0.8** **(0.05)**	- -	-0.2 (0.62)

Table S2. A summary of relationship between aerosol optical depth and light extinction coefficient measured by CAPS in four seasons.

	Entire	Spring	Summer	Fall	Winter
Effective Height (m, slope)	1233	1200	1800	964	635
r	0.64	0.66	0.76	0.72	0.72

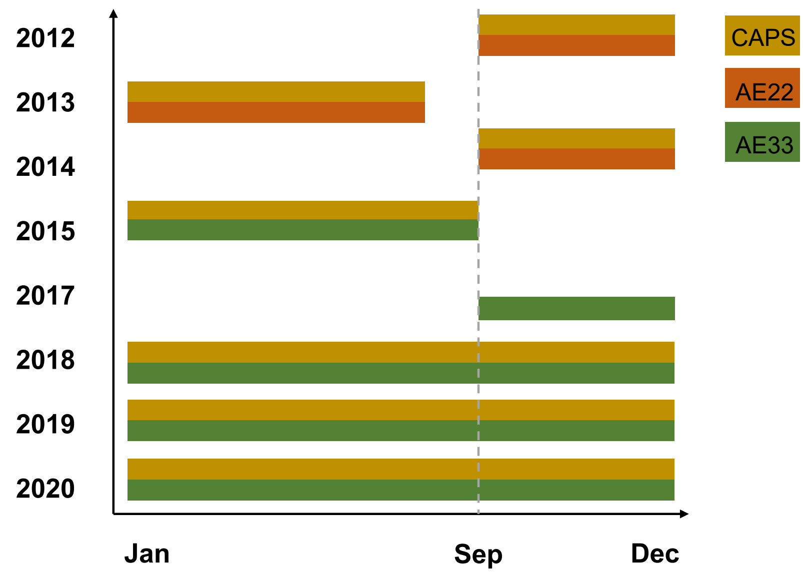

Fig. S1. Schematic representation of instrument deployment in different years.

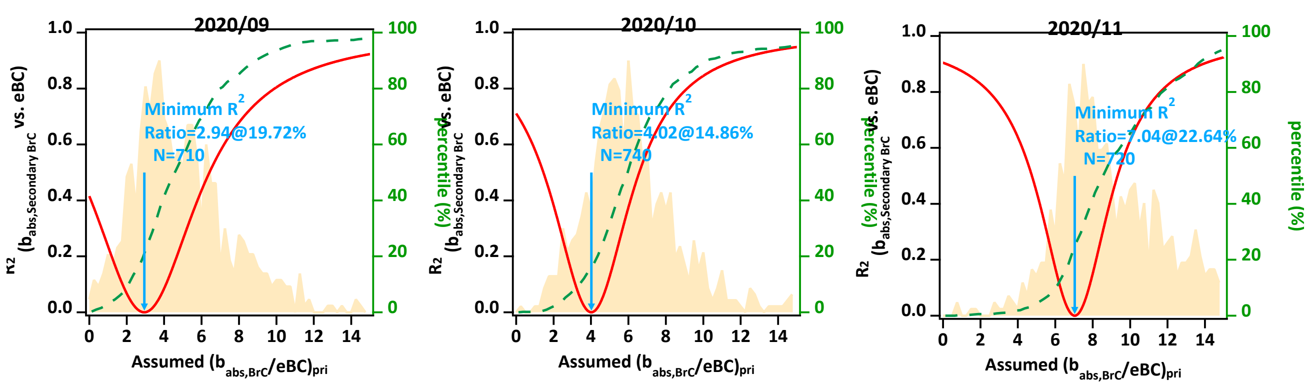

Fig. S2. ($b_{abs,\ BrC}$/eBC) $_{pri}$ determination by MRS at 370nm in September, October, November in 2020. The red line represents the correlation coefficient (R^2) between hypothetical $b_{abs,\ Secondary\ BrC}$ and eBC mass as a function of ($b_{abs,\ BrC}$/eBC) $_{pri\_h}$. The shaded area in light tan represents the frequency distribution of observed ($b_{abs,\ BrC}$/eBC) $_{pri}$. The dashed green line is the cumulative distribution of observed ($b_{abs,\ BrC}$/eBC) $_{pri}$.

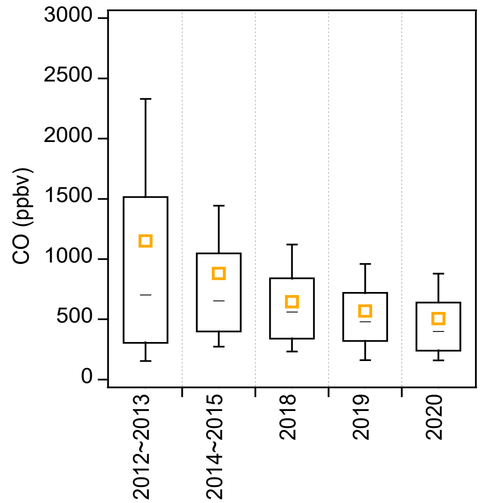

Fig. S3. Annual variation of CO concentration. The median (horizontal line), mean (square), 25th and 75th percentiles (lower and upper box), and 10th and 90th percentiles (lower and upper whiskers) are also shown, same as below.

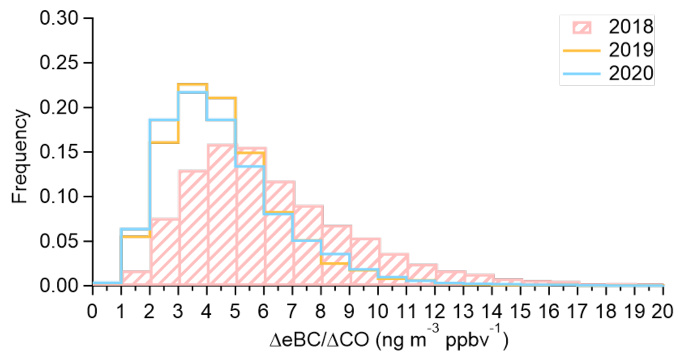

Fig. S4. The frequency distributions of △eBC/△CO in the past three years.

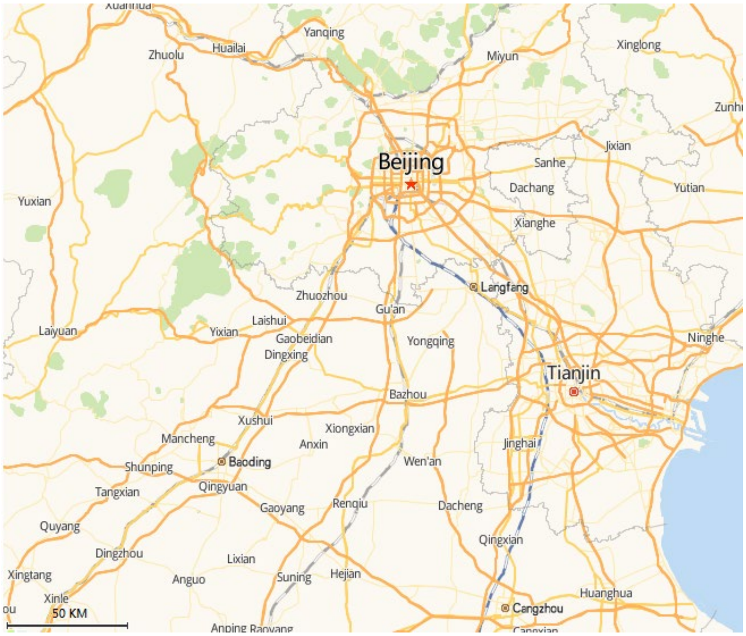

Fig. S5. Distribution of cities and towns around Beijing (© Google Maps).

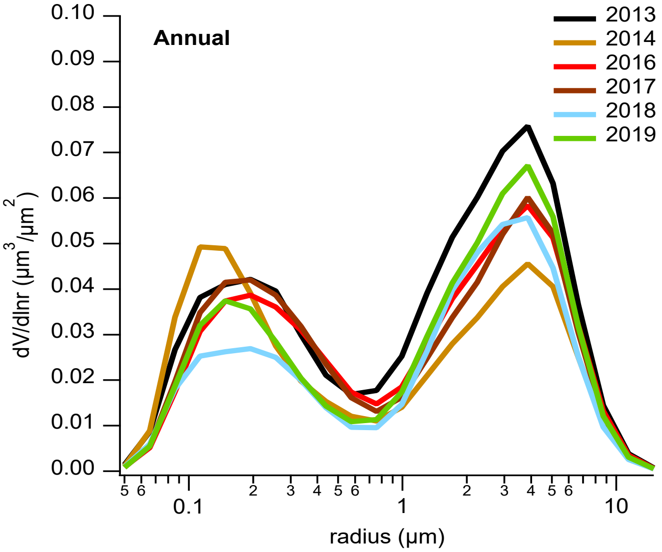

Fig. S6. Annual variations of aerosol volume size distribution in Beijing (available from the Aerosol Robotic Network data archive).

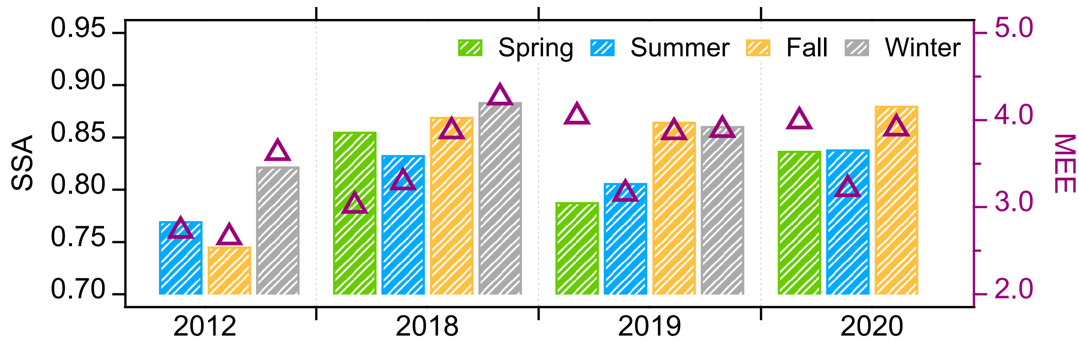

Fig. S7. Seasonal mean of SSA and MEE.

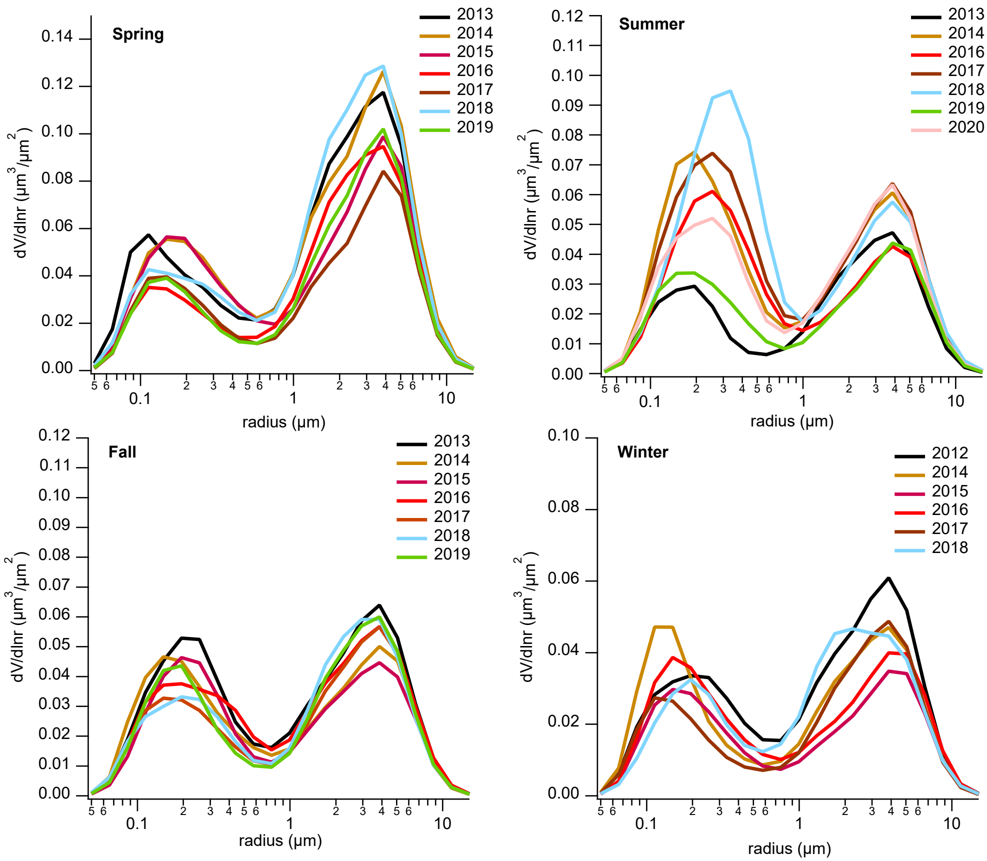

Fig. S8. Seasonal variations of aerosol volume size distribution in Beijing (available from the Aerosol Robotic Network data archive).

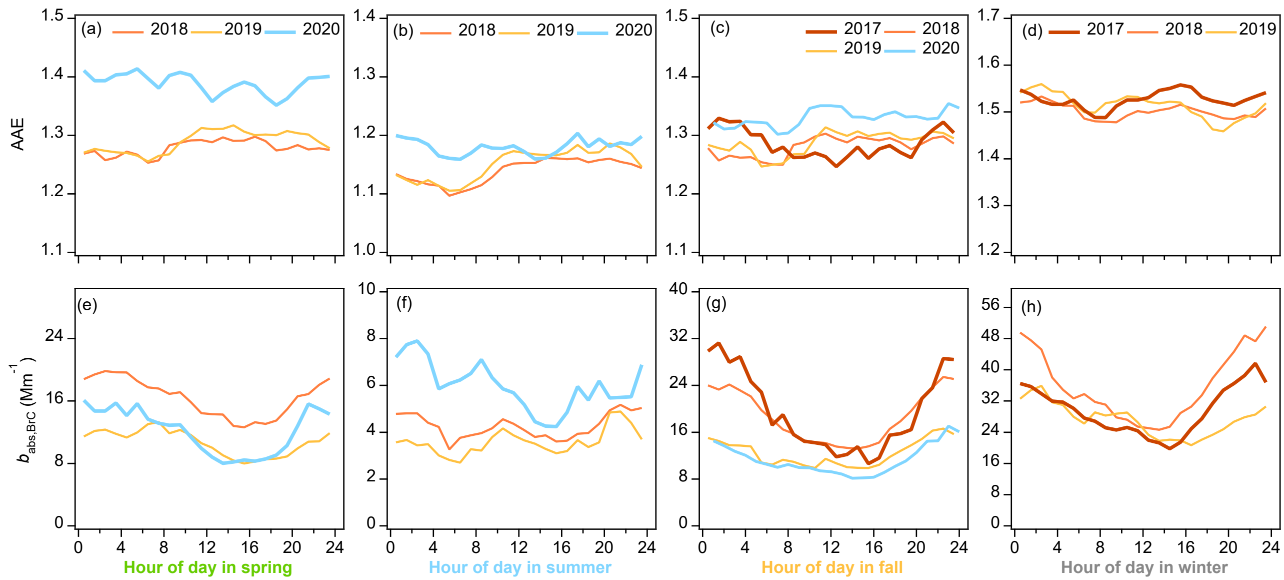

Fig. S9. Diurnal variations of AAE and $b_{abs,\ BrC}$ for spring, summer, fall and winter time in different years.

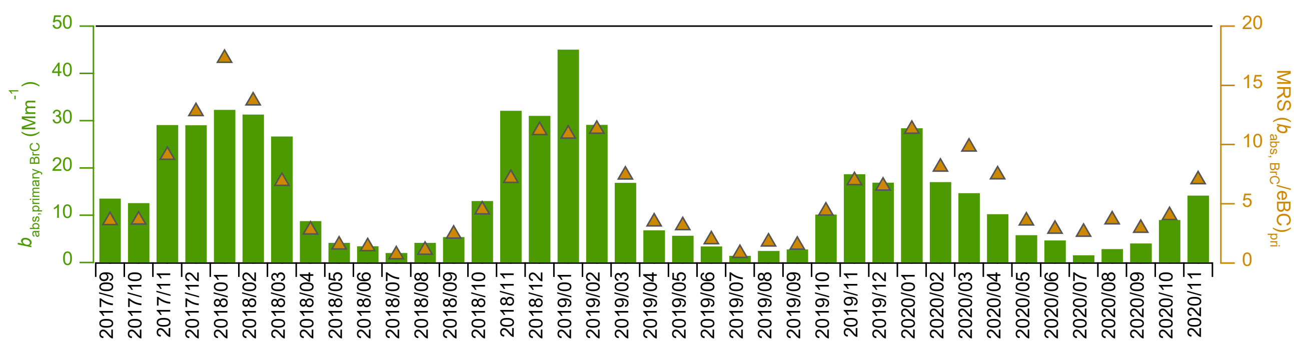

Fig. S10. Monthly variations in results of MRS and $b_{abs,\ primary\ BrC}$.

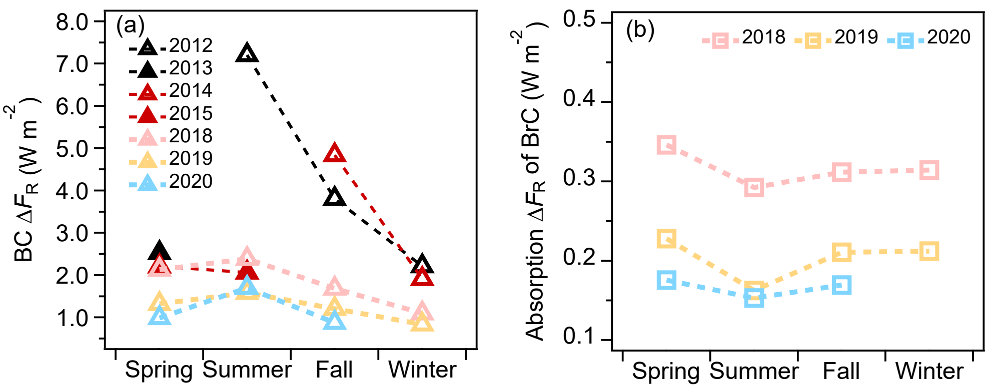

Fig. S11. Seasonal variations of BC ΔF_R and BrC absorption ΔF_R.

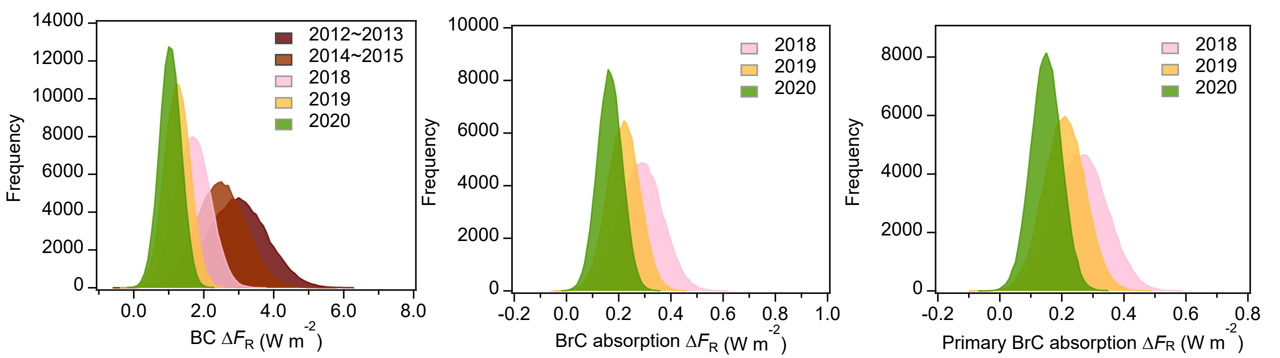

Fig. S12. Probability distributions of ΔF_R for BC, BrC and primary BrC based on 100,000 Monte Carlo simulations.

References

Bond, T. C., Doherty, S. J., Fahey, D. W., Forster, P. M., Berntsen, T., DeAngelo, B. J., Flanner, M. G., Ghan, S., Kärcher, B., Koch, D., Kinne, S., Kondo, Y., Quinn, P. K., Sarofim, M. C., Schultz, M. G., Schulz, M., Venkataraman, C., Zhang, H., Zhang, S., Bellouin, N., Guttikunda, S. K., Hopke, P. K., Jacobson, M. Z., Kaiser, J. W., Klimont, Z., Lohmann, U., P., S. J., Shindell, D., Storelvmo, T., Warren, S. G., and Zender, C. S.: Bounding the role of black carbon in the climate system: a scientific assessment, J. Geophys. Res.-Atmos., 118, 5380-5552, 10.1002/jgrd.50171, 2013.

Gyawali, M., Arnott, W. P., Lewis, K., and Moosmuller, H.: In situ aerosol optics in Reno, NV, USA during and after the summer 2008 California wildfires and the influence of absorbing and non-absorbing organic coatings on spectral light absorption, Atmos. Chem. Phys., 9, 8007-8015, 10.5194/acp-9-8007-2009, 2009.

Lack, D. A. and Langridge, J. M.: On the attribution of black and brown carbon light absorption using the Ångström exponent, Atmos. Chem. Phys., 13, 10535-10543, 10.5194/acp-13-10535-2013, 2013.

Lu, Z., Streets, D. G., Winijkul, E., Yan, F., Chen, Y., Bond, T. C., Feng, Y., Dubey, M. K., Liu, S., Pinto, J. P., and Carmichael, G. R.: Light absorption properties and radiative effects of primary organic aerosol emissions, Environ. Sci. Technol., 49, 4868-4877, 10.1021/acs.est.5b00211, 2015.